Catal Lett (2007) 119:191–198
DOI 10.1007/s10562-007-9227-1

Ethene Oxidation on Pd(111): Kinetic Hysteresis Induced by Carbon Dissolution

Harald Gabasch · Axel Knop-Gericke · Robert Schlögl · Werner Unterberger · Konrad Hayek · Bernhard Klötzer

Received: 26 March 2007 / Accepted: 19 July 2007 / Published online: 31 July 2007

Abstract The catalytic oxidation of ethene was studied on Pd(111) in the 10^{-7}–10^{-6} mbar pressure range by a molecular beam TPR hysteresis experiment between 400 K and 1,000 K. Two important effects were identified: the reaction-blocking effect of a dense chemisorbed adlayer of oxygen and the promotional effect of dissolved carbon segregating back to the surface and efficiently reducing the adsorbed oxygen. A strong dependence of the catalytic activity on the oxygen partial pressure is explained by the inhibiting effect of oxygen adsorption; high oxygen pressures in fact extinguish the reaction. The presence of oxygen-free metal surface area, where ethene can dissociate, is necessary for high activity. During heating the highest activity is observed at $T \sim 620$ K, where a combination of oxygen clean-off by carbon segregating back to the surface is combined with a high ethene adsorption rate, thus forming additional reaction sites *and* additional reaction products. During heating this carbon-induced clean-off of O(ad) is very efficient because the dissolved C atoms rather accumulate in the surface-near region and largely segregate back to the surface at $T > 600$ K. In contrast, during cooling from higher temperatures a high surface-near carbon bulk concentration does not build up because the bulk mobility of C atoms is also high and the faster diffusion of C into deeper layers counteracts carbon enrichment in the surface-near metal bulk. This effect favours a higher oxygen surface coverage and a stronger deactivation during cooling. If the carbon loading of the surface-near region was increased by decomposition of clean ethene prior to the reaction experiment, the promotional effect during the heating cycle was strongly enhanced, but the cooling cycle showed no memory of the C presaturation. Generally, the observed hysteresis effects stem from an interplay of combined oxygen site blocking and carbon diffusion effects.

Keywords Palladium · Dissolved carbon · Ethene oxidation · Kinetic hysteresis · Temperature programmed reaction · Reactive sticking probability

1 Introduction

Dispersed palladium metal is an important catalyst for hydrocarbon (in particular CH_4) combustion [1–3]. The catalytic activity and the well-known kinetic hysteresis effects [4–6] are associated with the formation and decay of the bulk PdO phase, and Pd is claimed to be most active in a highly oxidized state. On the other hand, palladium containing catalysts are also used in the selective oxidation of hydrocarbons, e.g. of ethene to acetaldehyde or to acetic acid [7–10], and of ethene plus acetic acid to vinyl acetate [11–13]. For these reactions, a more reduced state of the catalyst

Konrad Hayek—deceased.

H. Gabasch · A. Knop-Gericke · R. Schlögl
Abteilung Anorganische Chemie, Fritz-Haber-Institut der Max-Planck-Gesellschaft, Faradayweg 4-6, 14195, Berlin, Germany

H. Gabasch · W. Unterberger · K. Hayek · B. Klötzer (✉)
Institut für Physikalische Chemie, Universität Innsbruck, Innrain 52A, Innsbruck, 6020, Austria
e-mail: Bernhard.Kloetzer@uibk.ac.at

consisting of Pd metal modified by dissolved C atoms, is of importance [14].

Considerable knowledge exists about the interaction of Pd with unsaturated hydrocarbons because of their higher sticking probabilities compared to their saturated counterparts, allowing for a characterisation by various spectroscopic and microscopic techniques. The adsorption of clean ethene on Pd(111) at low temperature was investigated e.g. by infrared spectroscopy [15], electron energy loss spectroscopy [16], high resolution XPS and HREELS [17] and TPR [18]. Below 200 K ethene is molecularly adsorbed as a di-σ or π bonded species, while above 300 K it dissociates completely, forming ethylidyne on the surface and delivering H_2 to the gas phase. Up to about 350 K the C–C bond is not dissociated and the interaction of ethylidyne with the metal is limited to the surface. At temperatures beyond 410 K ethylidyne decomposes toward carbon, which starts to migrate into the bulk above 440 K, overcoming an activation barrier for C surface to subsurface diffusion of 107 kJ/mole [18].

From the work of Ziemecki et al. [19] it is known that Pd undergoes a phase transformation if the metal is exposed to carbon-containing gases like ethyne or ethene at atmospheric pressure above 423 K. The new phase is manifested by an expansion of the Pd unit cell and decomposes above 873 K in inert atmosphere. By analyzing the depth profiles of carbon these authors detected a diffusion front of carbon moving as a function of ethylene exposure and temperature.

The formation of carbonaceous residues and the partial dissolution of carbon in the Pd bulk affect both the decomposition and oxidation of carbon-containing molecules. Shaikhutdinov et al. [20] attempted to rationalize the effects of carbon deposits on small palladium particles on the adsorption of CO and ethene, while Bertarione et al. [21] observed that carbon contamination may influence the reaction pathway of methanol decomposition by blocking edge and defect sites on the particle surface. More detailed information about the composition and further reaction of CH_x overlayers was obtained in a high-pressure study by Morkel et al. [22], with help of vibrational sum frequency generation (SFG) and X-ray photoelectron spectroscopy (XPS). Some of the present authors observed that polycrystalline palladium exhibits its highest selectivity for partial oxidation of ethene to acetic acid at about 423 K [23], in the temperature range where ethylidyne mainly decomposes towards surface-adsorbed carbon atoms [18]. In [23] it was also shown that a pre-treatment of the Pd surface with 6 mbar ethene at 493 K, resulting in massive surface-near carbon accumulation, markedly enhanced the selectivity toward acetic acid. The formation of a subsurface PdC phase has also been shown to induce improved selectivity in pentyne hydrogenation toward pentene by inhibiting bulk-to-surface hydrogen diffusion [24].

The present paper is dedicated to the oxidation hysteresis of ethene on a Pd(111) surface. In particular, the influence of a preadsorbed 0.25 ML p(2 × 2) oxygen adlayer, of a pre-formed 2D Pd_5O_4 oxide layer [25], and of pre-dissolved carbon were investigated. It complements a parallel synchrotron in-situ XPS investigation of ethene oxidation performed in the 10^{-3} pressure range [26], which revealed the formation of a surface-near Pd_xC_y dissolved carbon phase at temperatures around 480 K. Due to the much higher reactant pressure used in study [26], only small concentrations of adsorbed oxygen and no surface oxides could be detected by in-situ XPS spectroscopy, and therefore their influence on the reaction kinetics remained to be clarified. Moreover, it is of interest that carbon accumulation in surface-near regions can take place in parallel with oxygen adsorption under rather lean conditions of a hydrocarbon oxidation reaction [13, 26], thus influencing activity and selectivity simultaneously.

2 Experimental

The UHV chamber for kinetic measurements was equipped with low-energy electron diffraction (LEED), Auger electron spectroscopy (AES), an effusive beam doser based on a capillary array for directional adsorption experiments (Galileo Optics, setup similar to that reported in [27]), and a differentially pumped quadrupole mass spectrometer (QMS) for line-of-sight detection of molecules desorbing from the central part (a 3 mm ø spot) of the Pd(111) face. The Pd(111) sample (12 mm ø, 3 mm thick) was oriented within 0.2° of the bulk (111) plane and cleaned by flashing to 1,250 K, sputtering with 700 eV Ar^+, flashing to 1,200 K, exposure to 5×10^{-7} mbar oxygen during cooling from 1,200 K to 600 K, and final annealing to 1,273 K. Cleanliness was checked by AES and temperature-programmed desorption of adsorbed oxygen or CO.

Calibration of beam fluxes was achieved by measurement of the pressure decrease in a differentially pumped gas dosing system by means of a MKS Baratron absolute pressure transducer [28]. A second QMS monitoring the pressure changes in the main chamber was used for reactive sticking measurements, making use of the King and Wells technique [29], and for the

temperature-programmed reaction experiments. In the chosen dosing geometry ~90% of the gas effusing from the doser hits the sample, and the accurate value of this fraction had to be determined by comparison of the initial sticking probabilities of O_2 with data from supersonic beam experiments [30]. The reaction rates to CO and CO_2 were independently calibrated by introducing a defined beam flux of CO and CO_2 into the UHV chamber directly after a complete TPR experiment. In this way the CO and CO_2 QMS signals induced by the reaction could be directly related to the calibration beam flux given in ML/s. Throughout this work, coverages and beam fluxes refer to 1 ML (monolayer) as a 1:1-ratio of oxygen or carbon atoms to 1.53×10^{19} Pd surface atoms m^{-2} in the (111) bulk-terminated geometry. An ethene beam flux of 0.19 ML/s corresponds to an effective pressure of 1×10^{-6} mbar at 300 K gas temperature. For the TPR experiments the crystal was heated at a constant rate (40 K/min) during exposure to an O_2—ethene reactant mixture in front of the capillary array doser, kept at the highest temperature (usually 973 K) for about 1 min, and then cooled down at the same rate.

3 Results and Discussion

3.1 Reactive Sticking Probability of Ethene on the Chemisorbed p(2 × 2) Oxygen Adlayer and the Pd_5O_4 Surface Oxide

In order to obtain direct information about the reactivity of these Pd(111)-oxygen surface structures, they were exposed to a constant ethene beam flux of 3×10^{-2} ML s^{-1} at a sample temperature of 413 K. The chemisorbed p(2 × 2) 0.25 ML oxygen adlayer was generated by exposure of clean Pd(111) to 500 L of $^{18}O_2$ at room temperature, whereas for obtaining the Pd_5O_4 surface oxide an exposure to 4,000 L of $^{18}O_2$ at 673 K and at a pressure of 1.5×10^{-5} mbar oxygen was used [28]. Isotope labelling of oxygen was necessary to distinguish between ethene and $^{12}C^{16}O$, having both mass 28, and to enhance the detection limit. The formation of both adlayers was experimentally confirmed by LEED and TDS.

Figure 1 displays the respective reactive sticking probabilities of ethene. On both the chemisorbed p(2 × 2) (Fig. 1a) and the Pd_5O_4 (Fig. 1b) surface the initial ethene adsorption rate is zero (time = 0), and increases autocatalytically. This observation suggests that no direct reaction of ethene with either the stoichiometric surface oxide or the saturated chemisorbed adlayer takes place. Rather, it points to a reaction mechanism starting at specific reactive sites, e.g. defects, which proceeds autocatalytically due to the increase of reduced surface oxide- or O(ads)- free surface, on which ethene can dissociate. The reactive sticking curve of Fig. 1b suggests a two-stage reaction mechanism, and we tentatively propose the formation of an intermediate hexagonal $(\sqrt{67} \times \sqrt{67})$R12.2° substoichiometric oxide structure, which was previously observed by STM during isothermal decomposition of the Pd_5O_4 surface oxide [31]. The main purpose of the experiments shown in Fig. 1 was to provide clear evidence for the reaction-blocking effect of both a complete p(2 × 2) and a complete surface oxide layer.

3.2 Kinetic Hysteresis at an Ethene:Oxygen Ratio of 1:3

At the considerably higher ethene beam flux used in the following TPR experiments the initially Pd_5O_4 surface oxide- or O(ads)- covered Pd(111) surface adapts very quickly to the reaction mixture, and it made no detectable difference whether the reaction was started from an O(ads)-, a surface oxide-modified or simply from an initially clean surface. As can be deduced from Fig. 1, it may take only about 100 s at a 0.12 ML/s ethene flux already at ~400 K to reduce the preadsorbed oxygen or oxide adlayers and to approach a common steady state of the catalyst surface, irrespective of its initial state (total duration of a TPR experiment ~1800 s).

The experiment shown in Fig. 2 was thus started from an initially clean Pd(111) sample. The left graph

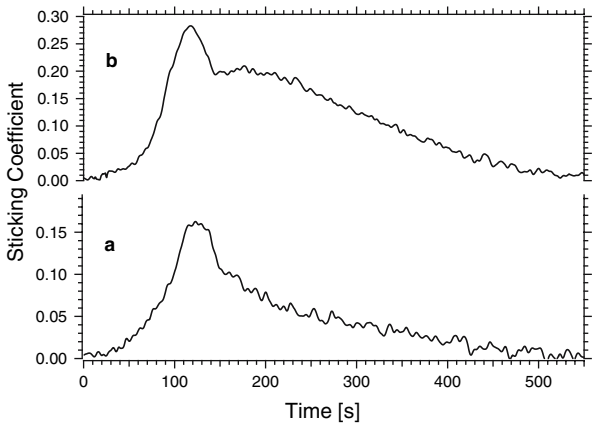

Fig. 1 Reactive sticking probability of a 0.12 ML s^{-1} ethene flux (**a**) on a complete chemisorbed p(2 × 2) adlayer (0.25 ML oxygen), (**b**) on a complete Pd_5O_4 2D surface oxide layer (0.58 ML oxygen)

of Fig. 2 shows the rate of CO formation as a function of the sample temperature during heating and cooling. The chosen reaction conditions were an ethene flux of 0.12 ML/s and an oxygen flux of 0.36 ML/s, i.e. a 1:3 reactant ratio, which leads to a particularly high reaction rate. The dominant reaction product is CO, and CO_2 formation remains at <10% throughout (see also Fig. 2, right side). During the heating cycle CO formation starts to increase at ~500 K, passes through a sharp maximum at 645 K, and then decreases again to reach a minimum at 770 K. Up to 973 K the CO formation rate increases again. After reaching 973 K, the sample temperature was kept constant for 1 min and was then reduced at the same rate (40 K min^{-1}). Between 973 K and ~800 K the reaction rate shows no hysteresis, i.e. it depends only on the temperature and is the same upon heating and cooling. Thereafter, the rate minimum during cooling occurs at a lower temperature, around 710 K, indicating a hysteresis in the reaction rate. This hysteresis is also clear from the smaller rate maximum appearing during the cooling cycle at a temperature of 575 K, which is 70 K lower than during heating.

Further information about the origin of the kinetic hysteresis can be derived by plotting the main involved species, CO, CO_2 and ethene, as a function of time, as shown in the right hand graph of Fig. 2. The water formation rate has been omitted as it follows exactly the trace of the ethene conversion in all experiments.

Ethene conversion starts already at ~450 K, prior to the onset of CO production, but precisely in the temperature range of beginning bulk migration of carbon [18] and passes a comparatively broad maximum already at 600 K. In comparison, CO production is shifted to higher temperature with a sharp maximum at 645 K (please mind the interpolation of the temperatures indicated in Fig. 2, right side). This observation suggests that during heating between 450 and 550 K, while CO formation is still low, the Pd surface-near region stores unreacted carbon, which remains for a while withdrawn from the oxidation on the surface. Increasing the temperature depletes this reservoir with some delay, delivering a part of the C atoms back to the surface, which causes an increased CO formation rate both because of reduced surface deactivation by oxygen and the extra amount of segregating carbon. The role of oxygen deactivation and the amount of surface-available dissolved carbon will be clarified in the context of Fig. 3, together with the explanation of the low-temperature shift of the smaller cooling rate maximum (left Fig. 2, cooling cycle). During cooling no hysteresis between ethene consumption and CO formation was observed and both species exhibit a maximum at 580 K (Fig. 2, right side).

Although the carbon storage scenario is a necessary ingredient for the explanation of the observed hysteresis, it cannot account for the sequence of maxima and minima in conversion and CO formation occurring *both* during heating *and* cooling. The rate maximum in the temperature range between 570 K and 650 K and the rate minimum between 700 and 750 K are observed in either direction, although to a varying degree and at different temperatures, and hence appear to be a general feature in the catalytic performance, irrespective of rate hysteresis. The kinetics of product formation will be at optimum at an optimum C and O coverage ratio on the surface which is apparently reached on Pd(111) at 600–650 K. If the surface temperature exceeds 650 K the bulk diffusion of C becomes very fast [18] and represents an additional rate contribution for removal of surface carbon available for product formation. On the other hand, O(ads) is stable up to 750 K, the onset temperature of oxygen desorption from a p(2 × 2) 0.25 ML oxygen adlayer [28]. Hence, between 650 and 770 K the composition of the surface adsorbate layer will rather change toward a dense p(2 × 2) O(ads) adlayer than toward C(ads). As will be shown in the following Fig. 3, we observed a complete deactivation of the catalyst at higher oxygen partial pressures, and we already showed that the

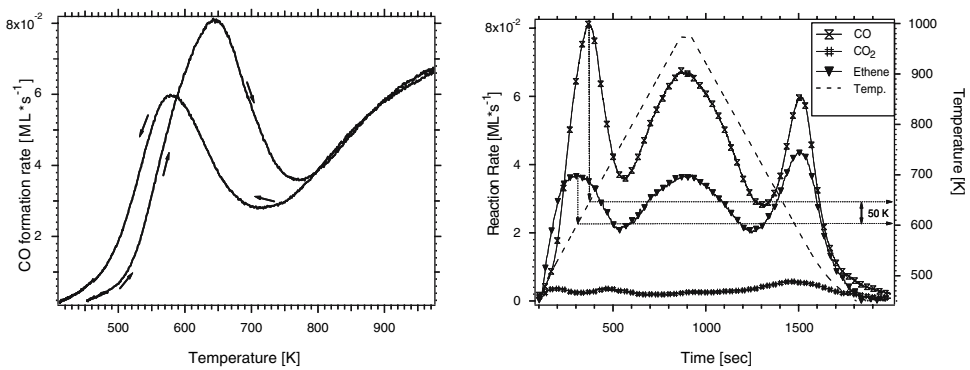

Fig. 2 Temperature programmed reaction during exposure to a C_2H_4/O_2 beam (1:3) based on an ethene flux of 0.12 ML s^{-1}, heating/cooling ramp 40 K min^{-1}. Left side: CO formation rate vs. temperature, showing the kinetic hysteresis; Right side: ethene conversion, CO-, CO_2 formation and temperature as a function of time

ethene reactive sticking on a complete p(2 × 2) oxygen adlayer is close to zero (Fig. 1). Hence, the more densely an O(ads) layer is packed, the stronger its deactivating effect becomes, most likely by blocking adsorption sites for ethene dissociation. Based on this concept we may distinguish certain temperature regimes where different, partially counteracting, processes become influential:

- During heating in the range between 450 and 550 K, while on-surface CO formation is still low, the surface-near bulk reservoir stores unreacted carbon. By approaching a temperature of ~650 K this reservoir is progressively released, either back to the surface or into deeper bulk regions. A part of the stored carbon can segregate back to the surface and become oxidized with O(ads) to CO, thereby reducing the mean oxygen surface concentration and creating additional adsorption sites for ethene. The 650 K heating rate maximum can therefore be rationalized on the basis of an optimum surface O(ads)/C(ads) ratio and extra CO formation originating from surface segregating C atoms.
- Above 660 K the bulk reservoir becomes emptied and the diffusion rate of C(ads) into the deeper bulk becomes fast, causing irreversible loss of C(ads). Consequently, the surface composition changes toward O(ads), leading to deactivation, and the reaction occurs mainly on the oxygen-covered metal surface at a reduced rate (~770 K).
- Remarkably, the rate starts to increase again above 770 K, close to the onset of oxygen desorption. Once this latter process becomes fast enough, more adsorption sites for ethene are again formed and the surface blocking is released.

This model can account for the existence of maxima in ethene conversion and CO formation both during heating and cooling. If the Pd bulk would be acting as an infinite and irreversible sink for C(ads) and C bulk migration would thus be completely "one-way" at all temperatures (i.e. the sample would not keep a partially reversible "memory" of its temperature- and time-dependent C loading), the rate maxima during heating and cooling would basically coincide and no rate hysteresis should be observed. However, it is likely that the hysteresis depends on the specific time- and T-dependent concentration profile of carbon perpendicular to the surface, its "carbon-memory". Upon heating C rather accumulates in surface-near regions, due to the reduced bulk diffusivity of carbon in the temperature range of accumulation, and thus a major part of the dissolved carbon has sufficient chance to diffuse back to the surface and to contribute to the reaction. The successive build-up and decay of a "steep carbon concentration profile" induces a shift of the maximum of CO evolution compared to ethene consumption, and an increased maximum rate at a somewhat higher temperature, as seen in Fig. 2. On the way down from high temperature the bulk has less possibility to accumulate carbon in surface-near regions because of its much higher diffusivity ("flat C profile"), and therefore the CO rate maximum is smaller and occurs also at lower T, this time coinciding with that of ethene consumption.

3.3 Kinetic Hysteresis at Different Ethene:Oxygen Ratios

For the TPR series of Fig. 3, an initially clean Pd(111) surface was exposed to a mixed molecular beam of ethene (0.12 ML/s) and $^{18}O_2$ using three different flux ratios of 1:3, 1:4 and 1:5. The CO formation rates resulting from these experiments are displayed in Fig. 3a–c. Heating and cooling again took place at a constant rate of 40 K min^{-1}. A higher oxygen:ethene ratio obviously leads to deactivation over the entire temperature range. At a 1:10 ratio the total rate approached zero and complete deactivation was observed up to 750 K (not shown). Moreover, the suppression of the rate maximum during the cooling cycle is even more pronounced at higher oxygen pressures, as can be best seen by its absence in trace c. This highlights also that the relative rate hysteresis between heating and cooling becomes strongly enhanced by a higher oxygen pressure (trace c). Finally, it is evident from a comparison of curves a, b and c that the position of both the heating and the cooling maxima is shifted to lower temperatures with increasing oxygen pressure (heating: from 635 K in (a) to 530 K in (c); cooling: from 565 K in (a) to 510 K in (b)).

According to our qualitative model introduced in Sect. 3.1, the predominance of oxygen adsorption relative to surface carbon adsorption is expected to be reached earlier (i.e. at a lower temperature) because of the increased oxygen adsorption rate, leading to a shift of the "region of rate decrease"—namely the region between the rate maximum and minimum, where the oxygen coverage increases relative to the carbon coverage—towards lower temperatures. This also implies that the rate minimum is approached at a lower temperature, which is evident from Fig. 3c (heating curve, ~630 K). Since the release of the surface blocking is only limited by the onset of oxygen desorption, which becomes fast above 750 K, the deactivation region, i.e. the region around the rate minimum, becomes broader.

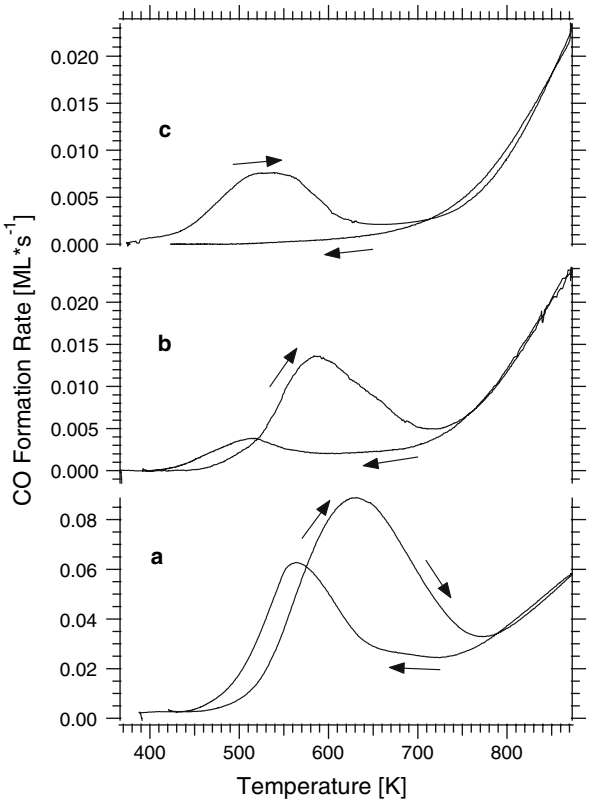

Fig. 3 CO formation rate during exposure to a C_2H_4/O_2 beam (1:3, 1:4, 1:5) based on an an ethene flux of 0.12 ML s^{-1} as a function of temperature; heating/cooling ramp 40 K min^{-1}

This can again be directly derived from the heating curves of Fig. 3a and c: the minimum region in (a) is quite narrow and located around 770 K, whereas it ranges from 600 K up to 750 K in (c). On this basis the shift of the rate maximum position, the broadening of the rate minimum and the overall deactivation can be qualitatively explained. During cooling at the 1:5 ratio (c) the deactivation by a dense chemisorbed oxygen adlayer cannot be released on the timescale of our experiment, most likely because of an efficient combination of the oxygen blocking of ethene adsorption and a reduced or absent contribution of dissolved carbon required for cleaning off the surface oxygen by surface segregation. Thus the cooling rate maximum is absent (Fig. 3c) or very weak (Fig. 3b)—the surface remains passivated.

3.4 Influence of Surface-near Carbon Presaturation

In order to examine the influence of additional dissolved carbon on CO evolution, we deliberately saturated the sample with carbon prior to the TPR experiment by a temperature-programmed pre-exposure to an ethene beam (flux 0.12 ML s^{-1}) for 1 h. We decreased the sample temperature in a stepwise manner every 15 min, from 573 K to 523, 473 and 443 K. This treatment resulted in the deposition of >80 ML of carbon in the surface-near region, as derived from the subsequent TPR experiment, which was performed under the same experimental conditions as in Figs. 2 and 3a (1:3-reactant ratio). The corresponding results with C presaturation are shown in Fig. 4 (left side: CO formation rate vs. temperature, right side: rates and temperature vs. time, CO_2 formation also included).

It is immediately obvious that the carbon stored near the crystal surface gives rise to a large quantity of additional CO formed during heating (~80 ML, obtained by integration of the area, compared to the cooling cycle), resulting in a broad peak with a maximum at 720 K. This clearly confirms the existence of a carbon-rich bulk region near to the surface which can deliver at least a part of the C atoms back to the surface. The absence of the typical rate minimum observed without previous C-saturation (Fig. 2, ~770 K), and the ongoing decrease of the rate even at the highest temperature of 973 K (held for 5 min, Fig. 4) suggest that the carbon segregation process can clean off the oxygen and contribute to additional CO formation up to the highest temperature used. The fact that the cooling curve closely coincides with its "C-unsaturated" reference experiment in Fig. 2 (left side) implies that the sample has finally lost its "carbon memory" after several minutes at the highest temperature (973 K).

Remarkably, ethene conversion (right side Fig. 4, dark triangles) starts simultaneously with CO formation at ~470 K, but then attains a constant level. Compared to the respective "not-presaturated" experiment (Fig. 2) the usual sequence of a rate maximum followed by a minimum is not observed. The considerations regarding blocked ethene adsorption by an O(ads) layer established at around 770 K can be easily applied to explain this behaviour. If the near-surface carbon reservoir is extensively rich, the diffusion of C atoms back to the surface occurs at a higher rate also at ~770 K and leads to a continuous removal of O(ads) by C(sub). Hence site blocking by O(ads) will be largely released and ethene adsorption and conversion stay at a high rate without passing through a minimum. The same holds for the missing minimum in the CO formation rate during heating in Fig. 4.

In contrast, during cooling O(ads)-induced deactivation is again observed, indicating that the whole quantity of surface-available dissolved C atoms was either consumed by oxidation or became lost in the

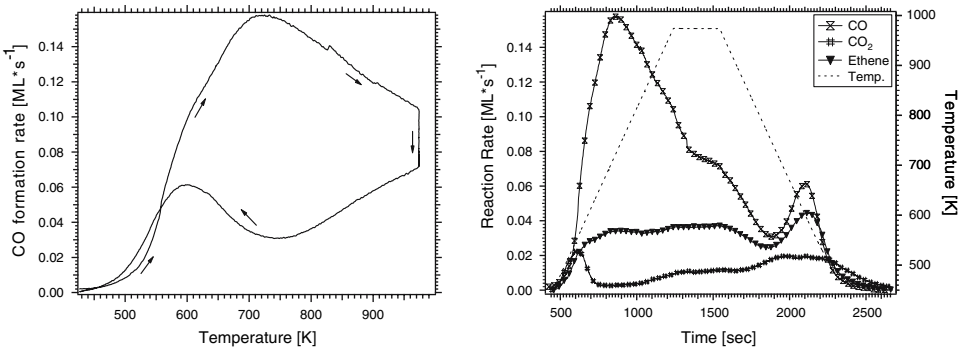

Fig. 4 Temperature programmed reaction performed as in Fig. 2, but after pre-exposure to 432 ML ethene between 573 K and 443 K sample temperature. C_2H_4/O_2 beam (1:3) based on a 0.12 ML s^{-1} ethene flux, heating/cooling ramp 40 K min^{-1}. Left side: CO formation rate vs. temperature; Right side: ethene conversion, CO formation, CO_2 formation and temperature vs. time

deeper sample regions during heating or during the 5 min period at 973 K.

The production of CO_2 is generally low (<10% relative to CO_2, see right side Fig. 4, rhombs). Significant amounts were observed during heating in the low-temperature range up to 600 K, most likely because chemisorption of CO is possible in this temperature region [32], favouring a secondary reaction of CO(ads) with O(ads) to CO_2. During cooling, CO_2 formation increases already at higher temperatures around 800 K, probably because the higher O(ads) coverage favours total oxidation.

Finally, the crystal was again presaturated with ethene in the same way as described for Fig. 4, and a TPR experiment was performed in clean oxygen (0.36 ML/s) without ethene (Fig. 5). The aim of this experiment was to measure the segregation kinetics of carbon without simultaneous external ethene supply and to assess the temperature region of beginning and maximum C segregation. The surface segregation of C again induces formation of CO and at low temperatures (<600 K) of CO_2 for the already discussed reasons. It starts at ~440 K, quite close to the temperature threshold of the reverse process, i.e. of C subsurface and bulk migration, as observed in [18], and reaches its maximum value at around 660 K. At temperatures above 660 K the CO rate decreases slowly, because of ongoing consumption of dissolved carbon depleting the surface-near reservoir. Nevertheless even at 1,273 K still some CO formation was observed, showing that the bulk was not completely depleted of C even at this very high temperature.

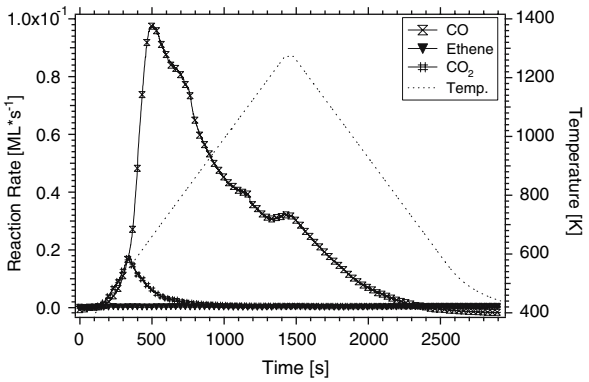

Fig. 5 Temperature programmed reaction after pre-exposure of clean Pd(111) to 432 ML ethene between 573 K and 443 K performed in a clean O_2 beam of 0.36 ML s^{-1}, heating/cooling ramp 40 K min^{-1}. Temperature and formation rates of CO and CO_2 plotted against time

4 Summary and Conclusions

In the present study of ethene oxidation on Pd(111) the influence of Pd surface or bulk oxide formation and decay can be excluded as the cause of kinetic hysteresis. The shape of the TPR traces and the position of the maxima remained unchanged if we started e.g. from a surface oxide covered surface. Additional LEED and TPD experiments did not show any hints of oxide formation during reaction. In our experiments we clearly identified carbon accumulation in the surface near region as the origin of the observed kinetic hysteresis.

These results are in obvious contrast to the total oxidation (combustion) of methane, both studied on supported and on bulk Pd catalysts. For the latter reaction, PdO, or rather "PdO_x" has been identified as the most active phase [5]. For a better understanding of the high PdO surface activity, a Mars-van Krevelen mechanism involving specific bridging oxygen species on top of both zirconia supported PdO, but also on bulk PdO, has been studied [33]. Some of the present authors recently studied methane oxidation on Pd(111)

by high-pressure in-situ XPS spectroscopy using synchrotron radiation, and found clear evidence that the formation of bulk PdO "seeds" on top of a surface-oxide covered Pd(111) sample induces strongly enhanced CH_4 oxidation activity, highlighting that highly dispersed PdO is the most active phase, even if formed on extended Pd bulk catalysts [34]. Moreover, it could be shown in [34] that—in the presence of rather high methane pressures—*no* detectable carbon dissolution into the Pd bulk occurred.

In contrast to the "PdO_x-promoted" methane total oxidation, the observed kinetic hysteresis of ethene oxidation on a bulk Pd(111) sample is based on activity differences *between the O(ad)-covered metal and the carbon-modified metal*, whereby a lowering of the oxygen coverage strongly promotes the reaction, in contrast to methane oxidation, where the reaction is promoted by an increasing oxygen content. During heating ethene adsorbs and decomposes on the metal surface and the resulting carbon deposits migrate into the surface near region at $T > 440$ K. The resulting "steep" C concentration profile facilitates further ethene adsorption by lowering the oxygen induced surface site blocking and additionally contributes to the maximum in CO formation during the heating stage. At higher temperatures the dissolved carbon becomes oxidized or lost into deeper regions of the sample, and the surface-near carbon reservoir becomes depleted, leaving behind an O(ads) covered surface exhibiting a lower activity, and finally an adsorbate-depleted metal surface with again increasing activity. During cooling, the higher C bulk diffusivity, together with the more efficient blocking by O(ads), leads to a "flat" C concentration profile and a reduced catalytic activity. The rate hysteresis shown in this work therefore results from a temperature- and time-dependent interplay of C dissolution, resegregation and O(ads) induced reaction blocking.

Acknowledgments H.G. acknowledges the German Max Planck Society for providing a research grant.

References

1. Lee JH, Trimm DL (1995) Fuel Process Technol 42:339
2. Kolaczowski ST (1995) Trans Inst Chem Eng 73:168
3. Heck RM, Farrauto RJ (2002) Catalytic air pollution control: commercial technology. Wiley, New York
4. Oh S, Mitchell P (1991) J Catal 132:187
5. Salomonsson P, Johansson S, Kasemo B (1995) Catal Lett 33:1
6. McCarty JG (1995) Catal Today 26:283
7. Xie J, Zhang Q, Chuang KT (2004) Catal Lett 93:181
8. Sano K, Uchida H, Wakabayashi S (1999) Catal Surv Jpn 3:55
9. Seoane JL, Boutry P, Montarnal R (1980) J Catal 63:191
10. Evnin AB, Rabo JA, Kasai PH (1973) J Catal 30:109
11. Stacchiola D, Calaza F, Burkholder L, Tysoe WT (2004) J Am Chem Soc 126:15384
12. Y-F Han, Kumar D, Sivadinarayana C, Clearfield A, Goodman DW (2004) Catal Lett 94:131
13. Y-F Han, Kumar D, Sivadinarayana C, Goodman DW (2004) J Catal 224:60
14. Bowker M, Morgan C, Perkins N, Holroyd R, Grillo FEF, MacDowall A (2005) J Phys Chem 109:2377
15. Kaltchev M, Thompson AW, Tysoe WT (1997) Surf Sci 391:145
16. Kesmodel LL, Gates JA (1981) Surf Sci 111:747
17. Sock M, Eichler A, Surnev S, Andersen JN, Klötzer B, Hayek K, Ramsey MG, Netzer FP (2003) Surf Sci 545:122
18. Gabasch H, Hayek K, Klötzer B, Knop-Gericke A, Schlögl R (2006) J Phys Chem B 110(10):4947
19. Ziemecki SB, Jones GA, Swartzfager DG, Harlow RL, Faber J Jr (1985) J Am Chem Soc 107:4547
20. Shaikhutdinov SK, Frank M, Bäumer M, Jackson S, Oldman RJ, Hemminger JC, Freund HJ (2002) Catal Lett 80:115
21. Bertarione JS, Scarano D, Zecchina A, Johanek V, Hoffmann J, Schauermann S, Libuda J, Rupprechter G, Freund H-J (2004) J Catal 223:64
22. Morkel M, Kaichev VV, Rupprechter G, Freund H-J, Prosvirin IP, Bukhtiyarov VI (2004) J Phys Chem B 108:12955
23. Unterberger W, Gabasch H, Hayek K, Klötzer B (2005) Catal Lett 104:1
24. Teschner D, Vass E, Hävecker M, Zafeiratos S, Schnörch P, Sauer H, Knop-Gericke A, Schlögl R, Chamam M, Wootsch A, Canning AS, Gamman JJ, Jackson SD, McGregor J, Gladden LF (2006) J Catal 242:26
25. Lundgren E, Kresse G, Klein C, Borg M, Andersen JN, Santis MD, Gauthier Y, Konvicka Ch, Schmid M (2002) Varga P, Phys Rev Lett 88:24
26. Gabasch H, Kleimenov E, Teschner D, Zafeiratos S, Hävecker M, Knop-Gericke A, Schlögl R, Zemlyanov D, Aszalos-Kiss B, Hayek K, Klötzer B (2006) J Catal (in press)
27. Bozack MJ, Muehlhoff L, Russell JN Jr, Choyke WJ, Yates JT Jr (1987) J Vac Sci Tech A 5:1
28. Leisenberger F, Koller G, Sock M, Surnev S, Ramsey M, Netzer FP, Klötzer B, Hayek K (2000) Surf Sci 445:380
29. King DA, Wells MG (1972) Surf Sci 29:454
30. Sjövall P, Uvdal P (1998) Chem Phys Lett 355:282
31. Gabasch H, Unterberger W, Hayek K, Klötzer B, Klein C, Schmid M, Varga P, Kresse G (2006) Surf Sci 600:205
32. Klötzer B, Unterberger W, Hayek K (2003) Surf Sci 232:142
33. Ciuparu D, Altman E, Pfefferle L (2001) J Catal 203:64
34. Gabasch H, Hayek K, Kloetzer B, Unterberger W, Kleimenov E, Teschner D, Zafeiratos S, Haevecker M, Knop-Gericke A, Schloegl R, Aszalos-Kiss B, Zemlyanov D (2007) J Phys Chem C 111(22):7957